



ARTICLE

Development and Application of a High-Volume Recycled Powder Solidifying Material for Waterworks Sludge

Xiang Deng¹, Sudong Hua^{1*}, Fan Xia², Yanfang Zhang², Dapeng Guo³, Xinxing Zhu³ and Defei Zhu³

¹College of Materials Science and Engineering, Nanjing Tech University, Nanjing, 211816, China

²China Construction Installation Group Nanjing Construction Co., Ltd., Nanjing, 210023, China

³Nanjing Pukou Urban and Rural Construction Group Co., Ltd., Nanjing, 211800, China

*Corresponding Author: Sudong Hua. Email: huasudong@126.com

Received: 05 April 2021 Accepted: 02 June 2021

ABSTRACT

Recycled powder (RP) is produced as a by-product during the process of recycling construction and demolition (C&D) wastes, presenting a low additional value. Using RP-based solidifying material can not only improve its utilization efficiency, but also reduce the cost of commercial solidifying materials. To date, this is the best solidifying material utilized to dispose the original waterworks sludge (OWS) with high moisture contents (60%), and the product could be used to fabricate non-fired bricks. This has become a new environment-friendly technology of “using waste to treat waste”. In this paper, the influence of different particle sizes and dosages of RP on the prepared solidifying material was studied. Besides, unconfined compression strength (UCS), volume stability, chemical composition, and heat of hydration, pore structure of the solidifying material were characterized. Then, non-fired bricks were prepared by using the solidifying material, recycled aggregate, and original waterworks sludge. The UCS and softening coefficient (SC) of the non-fired bricks were evaluated. As a result, the 28-day UCS of the solidifying material with optimal (M30) was 35.40 MPa, which could reach 84.37% of Portland cement (PC). The addition of RP increased the volume stability of the solidifying material. The addition of a large amount of RP reduced the heat flux and cumulative heat release of the solidifying material, while its porosity increased. The UCS of non-fired brick (NF20) in 28 days was 15.19 MPa and the SC after 28 days was 78.35%. In conclusion, the preparation of solidifying material using RP could be a promising approach and has a great potential in disposal of original waterworks sludge.

KEYWORDS

Recycled powder; solidifying material; original waterworks sludge; non-fired brick; unconfined compressive strength

1 Introduction

The world is in the era of the rapid development of infrastructure construction. Building materials are highly needed and heavily used, resulting in a large amount of construction and demolition (C&D) wastes. As the world's largest consumer of raw materials, construction industry consuming 40% of the planet's available natural resources on the planet annually, which goes against the idea of sustainable development [1–3]. Among all the areas, China has been considered to have the world's fastest-growing



construction and demolition industry, which generating nearly half of the demolition waste in the world [4,5]. Besides, the random dumping and disorderly landfill of C&D wastes may also cause secondary pollution to the environment. Producing recycled aggregate is the most effective way to solve this issue. The properties of recycled aggregate have been extensively studied, and the application of recycled aggregate is well-developed as well [6–9]. Additionally, a large amount of dust is generated as a by-product during the process of recycling. Dust with a particle size below 150 μm is referred to be made into recycled powder (RP), which accounts for about 20–35% of the total C&D wastes [10,11]. It may cause air and groundwater pollution if RP is not recovered properly. The government has enacted a series of environmental laws that limit the over-exploitation of natural resources, resulting in the rising of the prices of natural sand, and cement. RP, as a by-product in the process of C&D waste disposal, has a relatively stable market price but has been rarely studied. Therefore, the reuse of RP is imperative to improve its utilization efficiency. It can reduce the demand for natural resources.

Recently, researchers have explored the pozzolanic effect of RP on cement, and studied its potential in partially replacing cement as a compensating material. Sun et al. [12] studied the addition of RP to concrete as a cement substitute, indicating that RP could promote the hydration of cement. Turanli et al. [11] used different types of ground clay brick (GCB) and measured their activity indices. It was found that GCB could meet the strength activity requirement of American Society for Testing and Materials (ASTM) criteria when it was used to replace cement. Also, GCB effectively suppressed alkali-silicon reactions. Liu et al. [13] investigated the potential of concrete-clay brick hybrid recycled powder (CB-HRP) as a supplemental material and discussed the change of the concrete including fluidity, compressive strength, and microstructure. It was found that CB-HRP affected the strength of the fabricated concrete.

Studies on RP indicate that it has the potential to be used as a supplementary cementitious material. Therefore, a solidifying material can be rationally prepared from RP. So far, the commonly used materials for cementitious solidification are cement, lime, and fly ash, etc. [14]. However, they also have certain disadvantages. For example, lime has a poor water stability; solidified soil made from fly ash shows low mechanical strength; cement-based solidified soil using costs much higher [15]. From the perspective of resource-saving and environmental protection, the application of solid waste in industrial cementitious materials has been attracting the attentions of worldwide researchers. Gu et al. [16] developed a soil stabilizer for road subgrade based on original phosphogypsum, and the mass ratio of phosphogypsum to the entire stabilizer reached 60%. Wu et al. [17] used steel slag powder as a component in cement to form a new curing agent, and studied the strength degradation of the solidified soil in seawater. Hence, the re-purposing of solid waste can not only solve the problem of solid waste itself, but also reduce the cost of solidifying materials.

During water purification, sludge is always produced in waterworks. Since flocculants need to be added in this process, there are residual flocculants left in the sludge. If the moisture content of the sludge is low, the sludge is easy to coagulate and is difficult to disperse. Thus, the sludge with high moisture content is demanded [18]. There are several ways to comprehensively utilize waterworks sludge. One way is to use it as green soil [19] or adsorption material. It can also be used to remove pollutants in rivers or soil [20–24]. In addition, it can be used to prepare burning ceramsite [25] and sintered clay bricks [26,27]. Making sintered clay bricks emits greenhouse gases, polluting the environment. So, it is a good idea to use waterworks sludge to prepare non-fired bricks. However, in China, the main disposal method of waterworks sludge at the present stage is still to discard it into natural waters and landfills [28].

RP has been used to prepare solidifying material, and then solidifying material is used for dispose of original waterworks sludge (OWS). This is a new environment-friendly technology of “using waste to treat waste”. Due to the poor particle grading and low activity of recycled powder, its utilization rate is low. The original waterworks sludge has a high moisture content and contains a residual water treatment

agent, which makes it easy to agglomerate. As a solution, the RP in the solidifying material can effectively absorb the water in the sludge and disperse the sludge. In this paper, the influence of different particle sizes and dosages of RP was studied in order to prepare a solidifying material. Besides, properties of the solidifying material such as the unconfined compression strength, volume stability, chemical structure, heat of hydration, and pore structure were characterized. On this basis, a solidifying material was optimized and fabricated for the disposal of original waterworks sludge. Finally, the solidifying material, the recycled aggregate of C&D wastes and OWS were used to prepare non-fired bricks. Also, the UCS and SC of the non-fired bricks were tested. The preparation of solidifying material using RP could be a promising approach and has a great potential in disposal of original waterworks sludge.

2 Materials and Methods

2.1 Materials

The RP was obtained from a construction waste disposal company in suqian, Jiangsu, China. RP was collected from the fine dusts produced during the crushing process of recycled aggregate. The recycled aggregate was made by crushing waste concrete. In this paper, RP was divided into three types, namely, coarse powder (0–0.017 mm), medium powder (0–0.074 mm) and fine powder (0–0.035 mm). The Portland cement (PC) is the original 42.5 Portland cement produced by Anhui Conch Group Co., Ltd., China. The OWS used in the experiment was from a waterworks in Nanjing, Jiangsu Province, China. The water content of sludge was up to 60%. The chemical compositions of the three materials (RP, OWS, and PC) were detected by the X-ray fluorescence spectrometer before the experiment. The corresponding test results are shown in [Table 1](#).

Table 1: Chemical compositions of raw materials

Material	Component (%)							
	SiO ₂	Al ₂ O ₃	CaO	Fe ₂ O ₃	K ₂ O	MgO	Na ₂ O	LOI ¹
RP	41.07	10.16	23.84	3.76	1.90	2.76	1.04	13.53
OWS	44.39	21.78	1.84	6.56	2.32	2.30	1.28	16.69
PC	27.61	10.34	48.98	3.39	0.65	2.32	0.21	3.66

Note: 1. LOI (loss of ignition at 1000°C).

It can be seen from [Table 1](#) that the main component of RP is SiO₂ (41.07%), followed by CaO (23.84%) and Al₂O₃ (10.16%). Al mainly comes from the water treatment agents. [Fig. 1](#) presents a scanning electron microscope (SEM) image of RP, showing that RP has a rough and porous surface.

2.2 Sample Preparation

The mixing proportions of RP and PC by weight are shown in [Table 2](#). In this paper, three different particle sizes of RP were studied. The substitution rates of RP were 30%, 40%, 50%, and 60%, respectively. In [Table 2](#), C30 represents that the substitution rate of coarse RP (0–0.107 mm) is 30%. Based on the naming rules, M represents medium RP (0–0.074 mm) while F represents fine RP (0–0.035 mm).

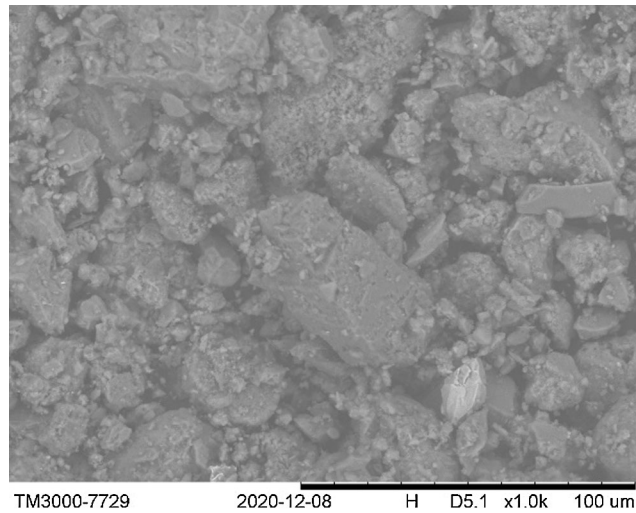


Figure 1: SEM image of RP

Table 2: Weight ratio of each raw material

Number	RP/%	PC/%	Water to binder ratio
F30	30/(0–0.107 mm)	70	0.35
F40	40/(0–0.107 mm)	60	0.35
F50	50/(0–0.107 mm)	50	0.35
F60	60/(0–0.107 mm)	40	0.35
M30	30/(0–0.074 mm)	70	0.35
M40	40/(0–0.074 mm)	60	0.35
M50	50/(0–0.074 mm)	50	0.35
M60	60/(0–0.074 mm)	40	0.35
C30	30/(0–0.035 mm)	70	0.35
C40	40/(0–0.035 mm)	60	0.35
C50	50/(0–0.035 mm)	50	0.35
C60	60/(0–0.035 mm)	40	0.35

According to the designated weight ratio in [Table 2](#), raw materials and water were weighed. First, a certain proportion of RP and PC were well mixed. Then a certain amount of water was poured into the container of a cement slurry mixer. Next, the well-mixed solidifying material was added to the cement slurry mixer. The mixture was slowly stirred for 2 min, and then quickly stirred quickly for another 2 min, resulting in the required slurry product. The water/solid ratio used in the study was 0.35. The slurry was cast into the 20 mm × 20 mm × 20 mm mold. Nine samples for each formula were prepared in total to test the UCS. After the samples were demoulded, they were placed in the standard curing box with a temperature of $20 \pm 2^\circ\text{C}$ and a humidity of 96%.

To test the volume stability of the samples, the prepared slurry was poured into 10 mm × 10 mm × 55 mm prismatic steel molds. To facilitate the measurement of the length of the samples, steel nails were installed at the ends of the molds before the slurry was cast.

Based on the result, the best formula of solidifying material was selected, and the solidifying material was used for disposal of OWS to prepare non-fired bricks. The solidifying material was stirred with the OWS and recycled aggregate (1–3 mm) for 30 s by using a cement mortar mixer. After thorough mixing by stirring, distilled water was added followed with another stirring for 2 min. Then the uniform mixture was placed in a mold (160 mm × 40 mm × 40 mm) and then molded with a press machine. After the sample was prepared, it was kept in a curing box at a constant temperature (20 ± 2°C) and humidity (96%). The specific experimental program is shown in Table 3. In Table 3, NF10 represents that the content of solidifying material in non-fired bricks is 10%. Other NF samples were named following the same naming rule. Different from NF ones, PC20 represents that the solidifying material is PC, and the dosage is 20%.

Table 3: Weight ratio of the raw materials in non-fired bricks

Number	Solidifying material/%	OWS/%	Recycled Aggregate (1–3 mm)/%	Water to the solidifying material/%
NF10	10	20	70	30
NF15	15	20	65	30
NF20	20	20	60	30
PC20	20	20	60	30
NF25	25	20	55	30

2.3 Test Methods

2.3.1 Unconfined Compressive Strength (UCS)

UCS was tested by a microcomputer-controlled automatic compression tester (WHY-200, Shanghai Hualong Test Instruments Corporation, Shanghai, China.). Three cubic samples (20 mm × 20 mm × 20 mm) cured with the same aging condition were tested. The average value of three test was identified as the UCS of the sample. The conditions of curing age were set as 3 days, 7 days, and 28 days. In parallel, the UCS test method of the non-fired bricks was the same as that of solidifying material, with curing ages of 7 days and 28 days.

2.3.2 Volume Stability

Volume stability tests were conducted on prismatic specimens with dimensions of 10 mm × 10 mm × 55 mm. After the slurry was cast, the sample was demoulded and the length of the sample was measured with a micrometer as the initial length L_0 . Then, the sample was maintained in a standardized curing box with a certain age, and the length of the sample was recorded as L_n . Finally, the volume change rate k_v of the sample was calculated according to Eq. (1).

$$k_v = \frac{L_n L_0}{55} \times 100\% \quad (1)$$

2.3.3 Crystalline Phase

The X-ray diffraction (XRD) test was carried out to characterize the crystalline phases in the solidifying material samples. The hardened samples were ground and then passed through a 200-mesh sieve. The powder sample was subjected to X-ray diffraction analysis (Rigaku-2500, Japan). An angular

range (5–55° 2θ) for scanning was used with a step interval of 0.02°, and a scan speed of 10°/min was set throughout the test.

2.3.4 Heat of Hydration

The heat of hydration was tested by isothermal conduction calorimetry (ICC). Heat of hydration was tested by TAM Air Isothermal calorimeter (Themmetric AB, Sweden). First, the was set to 20°C, then four gram of solidifying material were weighed (the water-to-binder ratio was set as 0.35). The solidifying material and water were added to the plastic bottle, stirred for 30 s, and then put the bottle into the isothermal calorimeter for continuous testing for 72 h.

2.3.5 Pore Structure

In order to obtain the details of the pore structure (pore size distribution and porosity), the samples were tested using a GT-60 mercury intrusion porosimeter (Kanta, USA) with both low- and high-pressure ports was used. Low- and high-pressure parameters range from 15–50 psi and 20–30000 psi, respectively. Before the test, the sample was crushed into a granular sample with a diameter of about 3 mm, and then dried at 60 ± 2°C for 4 h.

2.3.6 Softening Coefficient

The experiment was carried out by immersing the prepared non-fired brick samples (curing for 28 days) in the water for a while. When immersion time reached 7 days or 28 days, the sample was taken out of water, and the moisture on the surface was gently absorbed. The K_s of the sample was calculated according to Eq. (2):

$$K_s = \frac{f}{F} \times 100\% \quad (2)$$

where K_s stands for SC; f and F represent the UCS values of the sample before and after the immersion in water for a specified time, respectively.

3 Results and Discussion

3.1 Properties of the Solidifying Material

3.1.1 UCS

According to previous research, when the content of RP was less than 30%, the addition of RP could improve the mechanical properties of cement. With the increase of RP fineness, the mechanical properties were improved more obviously [29,30]. However, the further increase of RP content would have a negative effect on the mechanical properties. The UCS values of RP-based cements tested under different conditions including particle size and RP replacing percentage are presented in Fig. 2. As shown in Fig. 2, UCS values of the solidifying materials decreased as the replacement of RP increased. When the replacement amount of RP was increased from 30% to 40%, the UCS of coarse RP solidifying material at 28 days decreased by 22.50%. In contrast, UCS values of medium RP solidifying material and fine RP solidifying material dropped by 39.75% and 33.52%, respectively. However, less change in the UCS of the solidifying material was observed when the amount of RP substitution exceeded 50%. As the amount of RP increased in the solidifying material, the UCS decreased because there was a very little hydrated component in RP. RP could fill the void. However, when the amount of RP was too much, the filling effect was weakened due to the agglomeration effect of RP [29]. When the replacement of RP was 30%, solidifying material with medium size of RP showed highest UCS. The result can be explained as follows. When the particle size of RP decreased, the UCS of the solidifying material increased due to the filling effect. But when the particle size further decreased, the specific surface area of RP became larger.

The number of pores further increased so that it could adsorb free water in the solidifying material, resulting in the hindered hydration of cement [31].

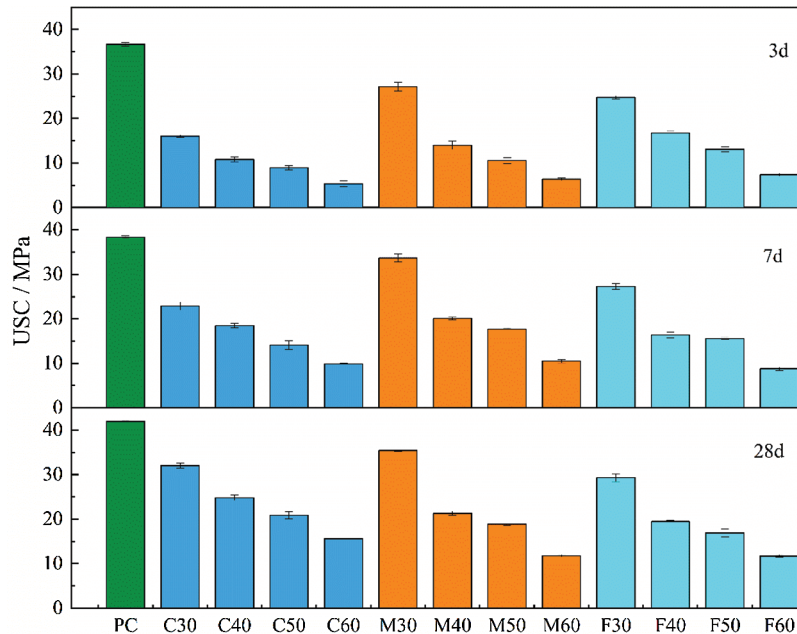


Figure 2: UCS values of the RP-based solidifying material with different conditions in terms of RP particle size replacing percentage and aging

3.1.2 Volume Stability

Fig. 3 shows the volume expansion rate trends of RP-containing paste. Based on a 60-day test, it can be seen from Fig. 3 that the specimens grew rapidly within the first 28 days, and then the expansion rate became constant during the second half of the test. The addition of RP can increase the volume stability of PC. With the increase of RP content, the volume of the sample was stabilized, and the expansion rate decreased gradually. One possible explanation is that the hydration of the sample was reduced due to the replacement of PC, which was similar to the effect of fly ash on shrinkage [32,33]. As a result, the expansion rates of RP-added pastes were lower than that of PC within 28 days. At 60 days, the expansion rate of C30 showed little difference from that of PC. And the expansion rate values of M30 and F30 were comparable, both less than that of PC. This may be attributed to the porous RP which absorbed the water. The finer RP could better fill the pore, reducing the expansion rate value [34]. The smaller expansion rate indicated a better volume stability of the sample. That explained why the M30 had a higher UCS.

3.1.3 XRD

Fig. 4 exhibits the XRD results of the solidifying materials with various RP additions. The main phases of the samples were quartz, portlandite, and calcite. Since the main phases of RP were calcite and quartz, so as the content of RP increased, the corresponding peaks in the solidifying materials also increased. In contrast, the portlandite content decreased with the increase of RP doping. One possible explanation is that there was a very little hydrated component in RP. With the increase of RP dosage, the hydration degree decreased, resulting in the decrease of portlandite content. In addition, the peaks of portlandite did not change significantly when the fineness of RP was changed. The results showed that RP barely participated in the hydrated reaction and tended to play a filling role.

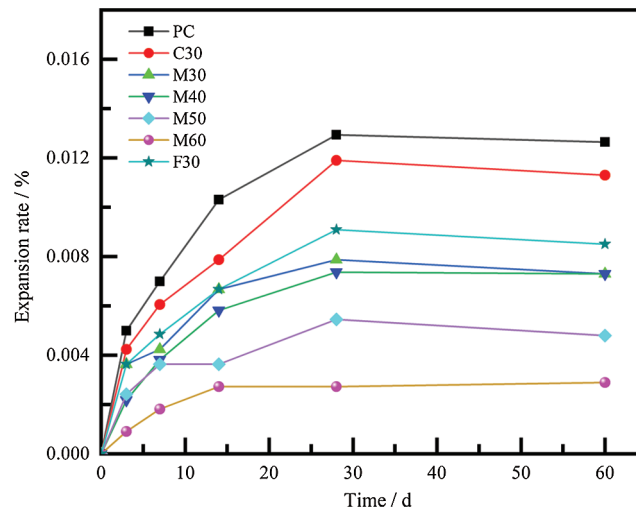


Figure 3: Expansion rates of different solidifying materials during aging

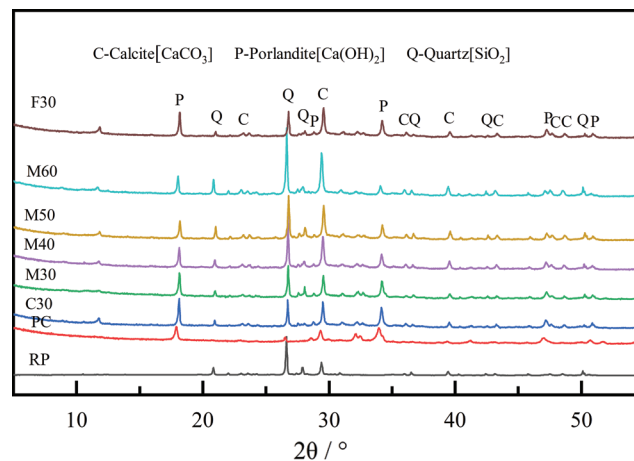


Figure 4: XRD patterns of RP, C30, M30-M60, and F30 solidifying materials curing in 28 days

3.1.4 Heat of Hydration

Fig. 5 shows the measurements of heat of hydration of the solidifying materials and PC. As shown in Fig. 5a, the heat flux of the solidifying material was reduced with the addition of RP. The large amount of substitution of RP resulted in a decreased hydrated component in the solidifying material, so the heat flux decreased. However, the peak of heat flux increased with the decrease of particle size. M30 reached the peak time of heat flux at about 15 h, which was the earliest, followed by F30 and C30. Since the hydration rate of C30 was slow in the early stage compared with M30 and F30, the strength of C30 was low in 3 d. One possible explanation is that the finer particles could better disperse the cement particles and increase the interface between cement and water [35,36]. According to the cumulative heat release curves in Fig. 5b, it can be found that the addition of RP increased the cumulative heat release of the solidifying material at the early stage. However, with a longer reaction time, the cumulative heat release values of RP-added pastes were lower than that of PC. M30 had the highest cumulative heat release except for PC, which agreed with the UCS result. Fig. 5c presents the heat flux of the first hour. F30 had higher heat flux than PC. This indicated that the heat of wetting (defined as the heat released per unit

mass of the initial dry powder when immersed in water) of fine RP was much higher than that of PC. The higher heat of wetting value it showed, the more porous the microstructure of the powder was. Thus, the result indicated that the structure of RP was more porous than PC [12,37]. The porous microstructure of the powder harmed the UCS of solidifying material. Therefore, when the particle size of RP decreased, the UCS of the solidifying material decreased.

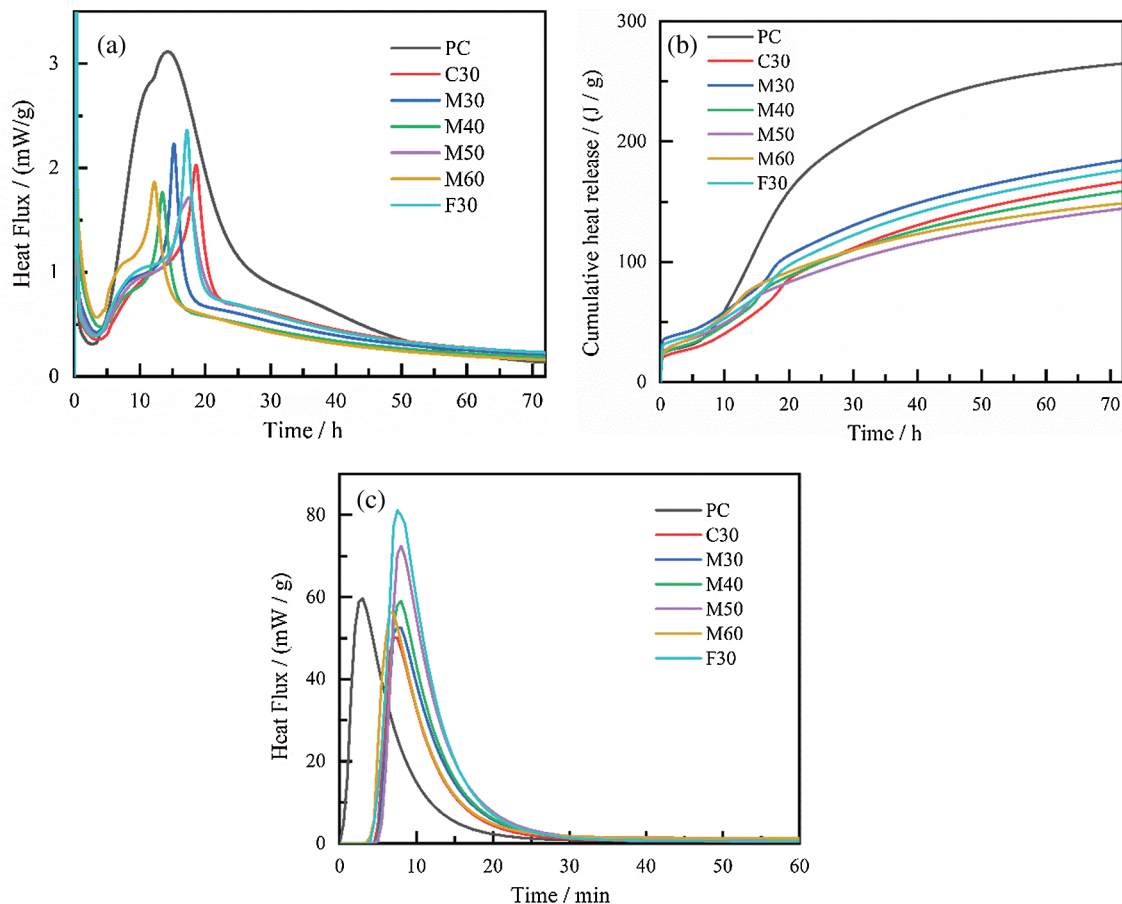


Figure 5: Heat of hydration of PC, C30, M30-M60, and F30. (a) Heat flux of 72 h; (b) cumulative heat release; (c) heat flux of the first hour

3.1.5 Pore Structure and Distribution

Fig. 6 shows the pore size distributions of five solidifying materials after 28 days of curing. The pores can be divided into three types: gel pores (<50 nm), pores (50–100 nm), and harmful macro-pores (>100 nm) [38,39]. It can be seen from Fig. 6 that the pore sizes of the C30, M30, F30, and PC were mainly distributed within a range of 10–50 nm, while the pore sizes of M40 are mainly in the range of 70–200 nm. The rough and porous surface of RP caused the main pore size of the solidifying material to be larger than that of PC. However, compared with C30 and F30, the main pore size of M30 was smaller. When the content of RP increased, the main pore size of the solidifying material become larger. Fig. 7 showed the porosity values of the solidifying materials and PC. Compared with PC, the porosity of M30 only increased by 7.43%, while that of C30 and F30 increased by 56.13% and 31.72%, respectively. Compared with M30, the porosity of M40 increased by 37.53%. Compared with C30, the porosity of M40 was slightly decreased, but the main pore size of M40 was larger. The XRD results showed that RP did not participate in the

hydrated reaction, mainly playing a filling effect. According to the results of porosity, the filling efficiencies of coarse powder and the fine powder were relatively lower, while that of medium powder was higher, which was consistent with the UCS test results.

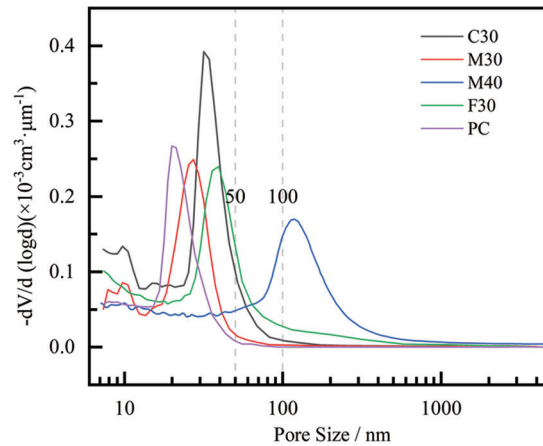


Figure 6: Pore size distribution of C30, M30, M40, F30, and PC at 28 days

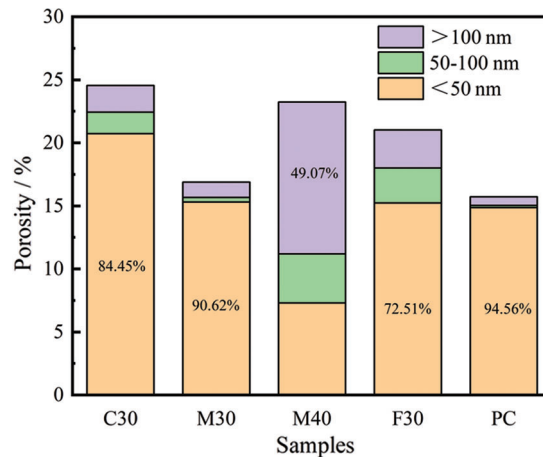


Figure 7: Porosity of C30, M30, M40, F30, and PC after curing for 28 days

3.2 Preparation of Non-Fired Bricks from OWS

Based on comprehensive evaluation of the UCS and volume stability of the solidifying materials, M30 showed the highest UCS and better volume stability. Hence, M30 was selected as the best formula.

To test the curing effect of the solidifying material, M30 was utilized as the solidifying material to prepare non-fired bricks, and was further compared with PC. Since too much OWS would have a great impact on the UCS of non-fired bricks, the proportion of OWS was set at 20%. Thus, the influence of solidifying material content on the UCS of non-fired bricks was studied. As a control group, the dosage of PC was also set at 20% during the experiment. The test results are shown in Fig. 8 and Table 4.

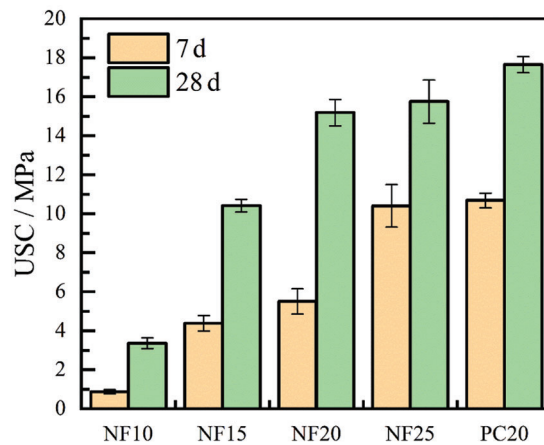


Figure 8: UCS values of non-fired bricks with different dosages of solidifying materials

Table 4: UCS and SC of NF20 and PC20

Sample	UCS/MPa		SC/K _s (%)	
	28 d	Soak 7 d	Soak 7 d	Soak 28 d
NF20	15.19	83.21	78.35	
PC20	16.52	86.83	85.18	

Fig. 8 shows the UCS values of non-fired bricks at 7 days and 28 days. According to Fig. 8, the UCS of the non-fired brick was increased with the increase of solidifying material content. When the solidifying material content was 20%, the UCS of the non-fired brick increased from 5.51 MPa (7 days) to 15.19 MPa (28 days) during aging. When the solidifying material content was increased to 25%, the UCS of non-fired brick in 7 days was nearly doubled, compared with that of NF20. However, according to the result at 28 days, the UCS of NF25 was only 3.69% higher than NF20. When the content of solidifying material was above 20%, the UCS of non-fired brick was not significantly improved. Compared with PC20, NF20 showed decreased UCS values at both 7 days (by 48.41%) and 28 days (by 13.94%). The UCS of NF20 was up to MU15 (GB/T 2542–2012 (in Chinese)). The increase in UCS of non-fired brick might be due to the increase of the solidifying material, which resulted in the increase of hydration products. The hydration products can fill the voids between the recycled aggregate of construction waste and OWS, resulting in the improvement of the strength. The OWS in the non-fired bricks competed for moisture with the solidifying material and hindered the hydration of the solidifying material. So the UCS was not significantly increased when a higher content of the solidifying material was used [40].

Table 4 shows the UCS and SC values of NF20 and PC20. It can be seen from the data that the SC of NF20 was 78.35% (28 d), which was 5.84% lower compared with that of 7 days. In contrast, the SC of PC20 reached 85.18% (28 d). The SC value was not significantly changed (only 1.92% lower than that on 7d). Compared with PC20, NF20 showed lower SC values at 7 and 28 days, which were 4.35% and 8.72% less, respectively.

Under China's existing environmental protection requirements, C&D waste and waterworks sludge are both general solid waste and are prohibited from being discharged at will. Since they have a potential risk of causing environmental pollution, a specialized enterprise is needed to dispose them. It costs about \$30 for

dispose of one cubic meter of sludge. If the sludge and C&D wastes are used for comprehensive utilization to prepare non-fired bricks, their utilization value could be improved.



Figure 9: (a) OWS; (b) OWS after mixed with solidifying material and recycled aggregates; (c) Non-fired bricks

4 Conclusions

In this paper, the effects of different particle sizes and dosages of RP on the UCS and volume stability of solidifying materials were studied. The phase element composition, heat of hydration, and pore structure of the solidifying material were characterized by XRD, ICC, and MIP. As a result, M30 was selected as an optimized solidifying material for OWS to prepare non-fired bricks. The UCS and SC of the fabricated non-fired bricks were evaluated. Based on the results of the experiments, the following conclusions can be drawn.

A large amount of RP would hurt the mechanical properties of the solidifying material since the UCS decreased with the increase of RP content. When the content of RP was above 30%, the smaller powder particles would harm the mechanical properties of the solidifying material. M30 showed the highest UCS (35.40 MPa at 28 days), which was still 15.63% lower compared with that of PC. The volume stability of the solidifying material was improved after the addition of RP.

The XRD results showed that RP did not participate in the hydrated reaction and only played a filling role. The results of the heat of hydration showed that the heat flux of paste was reduced by the addition of RP. M30 had the maximum cumulative hydration heat except for PC, indicating that M30 had the highest extent of hydration, which agreed with the large UCS value.

The results of the pore structure showed that the porosity of the solidifying material was increased by adding a large amount of RP. Compared with PC, the porosity of C30, M30, and F30 increased by 56.13%, 7.43%, and 31.72%, respectively. The result indicated that the filling effect would be weakened with the increase of finer powder content in RP.

Finally, M30 was selected as the solidifying material for OWS to prepare non-fired bricks. The UCS of NF20 was 15.19 MPa at 28 days. The 28-day SC of NF20 was 78.35%. Although a little sacrifice in the mechanical property was observed, the performance of NF20 non-fired bricks was still comparable to that of PC20. In conclusion, the preparation of solidifying material using RP could be a promising approach to improve the utilization efficiency of C&D wastes, which has a great potential in disposal of original waterworks sludge.

Acknowledgement: The authors would like to thank TopEdit (www.topeditsci.com) for linguistic assistance during preparation of this manuscript.

Funding Statement: This work was supported by the Jiangsu Provincial Science and Technology Department's Social Development-Major Science and Technology Demonstration Project (Grant No. BE2018697), the Demonstration Engineering Technology Research Center of Suqian Science and Technology Bureau (Grant No. M201912) and a Project Funded by the Priority Academic Program Development of Jiangsu Higher Education Institutions.

Conflicts of Interest: The authors declare that they have no conflicts of interest to report regarding the present study.

References

1. Hossain, M. U., Ng, S. T., Antwi-Afari, P., Amor, B. (2020). Circular economy and the construction industry: Existing trends, challenges and prospective framework for sustainable construction. *Renewable and Sustainable Energy Reviews*, 130, 109948. DOI 10.1016/j.rser.2020.109948.
2. Ruiz, L. A. L., Ramón, X. R., Domingo, S. G. (2020). The circular economy in the construction and demolition waste sector—A review and an integrative model approach. *Journal of Cleaner Production*, 248, 119238. DOI 10.1016/j.jclepro.2019.119238.
3. Pacheco-Torgal, F. (2017). High tech startup creation for energy efficient built environment. *Renewable and Sustainable Energy Reviews*, 71, 618–629. DOI 10.1016/j.rser.2016.12.088.
4. Wang, X. P., Yu, R., Shui, Z. H., Song, Q. L., Liu, Z. et al. (2019). Optimized treatment of recycled construction and demolition waste in developing sustainable ultra-high performance concrete. *Journal of Cleaner Production*, 221, 805–816. DOI 10.1016/j.jclepro.2019.02.201.
5. Yuan, H. P. (2017). Barriers and countermeasures for managing construction and demolition waste: A case of Shenzhen in China. *Journal of Cleaner Production*, 157, 84–93. DOI 10.1016/j.jclepro.2017.04.137.
6. Kisku, N., Joshi, H., Ansari, M., Panda, S. K., Nayak, S. et al. (2017). A critical review and assessment for usage of recycled aggregate as sustainable construction material. *Construction and Building Materials*, 131, 721–740. DOI 10.1016/j.conbuildmat.2016.11.029.
7. Marinkovic, S., Dragas, J., Ignjatovic, I., Tomic, N. (2017). Environmental assessment of green concretes for structural use. *Journal of Cleaner Production*, 154, 633–649. DOI 10.1016/j.jclepro.2017.04.015.
8. Thomas, J., Thaickavil, N. N., Wilson, P. M. (2018). Strength and durability of concrete containing recycled concrete aggregates. *Journal of Building Engineering*, 19, 349–365. DOI 10.1016/j.job.2018.05.007.
9. Tam, V. W. Y., Soomro, M., Evangelista, A. C. J. (2018). A review of recycled aggregate in concrete applications (2000–2017). *Construction and Building Materials*, 172, 272–292. DOI 10.1016/j.conbuildmat.2018.03.240.
10. Xiao, J. Z., Li, W. G., Sun, Z. H., Lange, D. A., Shah, S. P. (2013). Properties of interfacial transition zones in recycled aggregate concrete tested by nanoindentation. *Cement and Concrete Composites*, 37, 276–292. DOI 10.1016/j.cemconcomp.2013.01.006.
11. Turanli, L., Bektas, F., Monteiro, P. J. M. (2003). Use of ground clay brick as a pozzolanic material to reduce the alkali–silica reaction. *Cement and Concrete Research*, 33(10), 1539–1542. DOI 10.1016/s0008-8846(03)00101-7.
12. Sun, Z. H., Liu, F. J., Tong, T., Qi, C. Q., Yu, Q. (2017). Hydration of concrete containing hybrid recycled demolition powders. *Journal of Materials in Civil Engineering*, 29(7), DOI 10.1061/(asce)mt.1943-5533.0001842.
13. Liu, Q., Tong, T., Liu, S. H., Yang, D. Z., Yu, Q. (2014). Investigation of using hybrid recycled powder from demolished concrete solids and clay bricks as a pozzolanic supplement for cement. *Construction and Building Materials*, 73, 754–763. DOI 10.1016/j.conbuildmat.2014.09.066.

14. Ma, J. L., Zhao, Y. C., Wang, J. M., Wang, L. (2010). Effect of magnesium oxychloride cement on stabilization/solidification of sewage sludge. *Construction and Building Materials*, 24(1), 79–83. DOI 10.1016/j.conbuildmat.2009.08.011.
15. Huang, S., Lyu, Y. J., Peng, Y. J. (2020). Application research of New cementitious composite materials in saline soil subgrade aseismic strengthening. *Advances in Civil Engineering*, 2020, 7525692. DOI 10.1155/2020/7525692.
16. Gu, Z. H., Fang, A. G., Hua, S. D., Zhao, Q. Z., Sun, L. D. et al. (2021). Development of a soil stabilizer for road subgrade based on original phosphogypsum. *Journal of Renewable Materials*, 9(2), 253–268. DOI 10.32604/jrm.2021.011912.
17. Wu, Y. K., Shi, K. J., Yu, J. L., Han, T., Li, D. D. (2020). Research on strength degradation of soil solidified by steel slag powder and cement in seawater erosion. *Journal of Materials in Civil Engineering*, 32(7), 4020181. DOI 10.1061/(asce)mt.1943-5533.0003205.
18. Zhao, Y. Q., Nzihou, A., Ren, B. M., Lyczko, N., Shen, C. et al. (2020). Waterworks sludge: An underrated material for beneficial reuse in water and environmental engineering. *Waste and Biomass Valorization*, DOI 10.1007/s12649-020-01232-w.
19. Ng, S. L., Chu, L. M., Chan, S. H., Ma, A. T. H. (2020). The potential use of waterworks sludge in greening: A bioassay with bermudagrass [*Cynodon dactylon* (L.) pers.]. *Urban Forestry & Urban Greening*, 55, 126856. DOI 10.1016/j.ufug.2020.126856.
20. Cheng, G., Li, Q. H., Su, Z., Sheng, S., Fu, J. (2018). Preparation, optimization, and application of sustainable ceramsite substrate from coal fly ash/waterworks sludge/oyster shell for phosphorus immobilization in constructed wetlands. *Journal of Cleaner Production*, 175, 572–581. DOI 10.1016/j.jclepro.2017.12.102.
21. Lima, E. C., Naushad, M., Faisal, A. A. H., Naji, L. A., Al-Juhaishi, M. R. et al. (2020). Synthesis of composite sorbent for the treatment of aqueous solutions contaminated with methylene blue dye. *Water Science and Technology*, 81(7), 1494–1506. DOI 10.2166/wst.2020.241.
22. Ren, B. M., Lyczko, N., Zhao, Y. Q., Nzihou, A. (2020). Alum sludge as an efficient sorbent for hydrogen sulfide removal: Experimental, mechanisms and modeling studies. *Chemosphere*, 248, 126010. DOI 10.1016/j.chemosphere.2020.126010.
23. Shrestha, S., Kulandaivelu, J., Sharma, K., Jiang, G. M., Yuan, Z. G. (2020). Effects of dosing iron- and alum-containing waterworks sludge on sulfide and phosphate removal in a pilot sewer. *Chemical Engineering Journal*, 387, 124073. DOI 10.1016/j.cej.2020.124073.
24. Wang, L., Zou, F. L., Fang, X. L., Tsang, D. C. W., Poon, C. S. et al. (2018). A novel type of controlled low strength material derived from alum sludge and green materials. *Construction and Building Materials*, 165, 792–800. DOI 10.1016/j.conbuildmat.2018.01.078.
25. Monteiro, S. N., Alexandre, J., Margem, J. I., Sánchez, R., Vieira, C. M. F. (2008). Incorporation of sludge waste from water treatment plant into red ceramic. *Construction and Building Materials*, 22(6), 1281–1287. DOI 10.1016/j.conbuildmat.2007.01.013.
26. Cheng, W. N., Yi, H., Yu, C. F., Wong, H. F., Wang, G. X. et al. (2019). Biorefining waste sludge from water and sewage treatment plants into Eco-construction material. *Frontiers in Energy Research*, 7, 22. DOI 10.3389/fenrg.2019.00022.
27. Anderson, M., Elliott, M., Hickson, C. (2002). Factory-scale proving trials using combined mixtures of three by-product wastes (including incinerated sewage sludge ash) in clay building bricks. *Journal of Chemical Technology and Biotechnology*, 77(3), 345–351. DOI 10.1002/jctb.593.
28. Wang, Y. N., Yang, J. H., Xu, H., Liu, C. W., Shen, Z. et al. (2019). Preparation of ceramsite based on waterworks sludge and Its application as matrix in constructed wetlands. *International Journal of Environmental Research and Public Health*, 16(15), 2637. DOI 10.3390/ijerph16152637.
29. He, X. Y., Zheng, Z. Q., Yang, J., Su, Y., Wang, T. W. et al. (2020). Feasibility of incorporating autoclaved aerated concrete waste for cement replacement in sustainable building materials. *Journal of Cleaner Production*, 250, 119455. DOI 10.1016/j.jclepro.2019.119455.

30. Ma, Z. M., Tang, Q., Wu, H. X., Xu, J. G., Liang, C. F. (2020). Mechanical properties and water absorption of cement composites with various fineness and contents of waste brick powder from C&D waste. *Cement and Concrete Composites*, 114, 103758. DOI 10.1016/j.cemconcomp.2020.103758.
31. Liu, Q., Li, B., Xiao, J. Z., Singh, A. (2020). Utilization potential of aerated concrete block powder and clay brick powder from C&D waste. *Construction and Building Materials*, 238, 117721. DOI 10.1016/j.conbuildmat.2019.117721.
32. Lee, H. K., Lee, K. M., Kim, B. G. (2003). Autogenous shrinkage of high-performance concrete containing fly ash. *Magazine of Concrete Research*, 55(6), 507–515. DOI 10.1680/macr.55.6.507.37600.
33. Tertnkhajornkit, P., Nawa, T., Nakai, M., Saito, T. (2005). Effect of fly ash on autogenous shrinkage. *Cement and Concrete Research*, 35(3), 473–482. DOI 10.1016/j.cemconres.2004.07.010.
34. Gyurko, Z., Jankus, B., Fenyvesi, O., Nemes, R. (2019). Sustainable applications for utilization the construction waste of aerated concrete. *Journal of Cleaner Production*, 230, 430–444. DOI 10.1016/j.jclepro.2019.04.357.
35. Ma, Z. M., Liu, M., Duan, Z. H., Liang, C. F., Wu, H. (2020). Effects of active waste powder obtained from C&D waste on the microproperties and water permeability of concrete. *Journal of Cleaner Production*, 257, 120518. DOI 10.1016/j.jclepro.2020.120518.
36. Duan, Z. H., Hou, S. D., Xiao, J. Z., Li, B. (2020). Study on the essential properties of recycled powders from construction and demolition waste. *Journal of Cleaner Production*, 253, 119865. DOI 10.1016/j.jclepro.2019.119865.
37. Yu, K. Q., Zhu, W. J., Ding, Y., Lu, Z. D., Yu, J. T. et al. (2019). Micro-structural and mechanical properties of ultra-high performance engineered cementitious composites (UHP-eCC) incorporation of recycled fine powder (RFP). *Cement and Concrete Research*, 124, 105813. DOI 10.1016/j.cemconres.2019.105813.
38. Chen, X. D., Wu, S. X., Zhou, J. K. (2014). Experimental study and analytical model for pore structure of hydrated cement paste. *Applied Clay Science*, 101, 159–167. DOI 10.1016/j.clay.2014.07.031.
39. Zeng, Q., Li, K. F., Fen-Chong, T., Dangla, P. (2012). Pore structure characterization of cement pastes blended with high-volume fly-ash. *Cement and Concrete Research*, 42(1), 194–204. DOI 10.1016/j.cemconres.2011.09.012.
40. He, X. X., Chen, Y. J., Tan, X., Wang, S. Q., Liu, L. (2020). Determining the water content and void ratio of cement-treated dredged soil from the hydration degree of cement. *Engineering Geology*, 279, 105892. DOI 10.1016/j.enggeo.2020.105892.